frontiers | Frontiers in Earth Science

TYPE Original Research
PUBLISHED 04 July 2023
DOI 10.3389/feart.2023.1062916

OPEN ACCESS

EDITED BY
Matteo Picozzi,
University of Naples Federico II, Italy

REVIEWED BY
R. B. S. Yadav,
Kurukshetra University, India
Inessa Vorobieva,
Institute of Earthquake Prediction Theory and Mathematical Geophysics (RAS), Russia

*CORRESPONDENCE
Abhey Ram Bansal,
abhey.bansal@gmail.com

RECEIVED 06 October 2022
ACCEPTED 19 June 2023
PUBLISHED 04 July 2023

CITATION
Dixit M and Bansal AR (2023), The absence of remotely triggered seismicity in Gujarat, NW India during the Nepal earthquake, 2015.
Front. Earth Sci. 11:1062916.
doi: 10.3389/feart.2023.1062916

The absence of remotely triggered seismicity in Gujarat, NW India during the Nepal earthquake, 2015

Mayank Dixit[1] and Abhey Ram Bansal[2]*

[1]Institute of Seismological Research (ISR) Raisan, Gandhinagar, India, [2]CSIR National Geophysical Research Institute, Hyderabad, India

Gujarat in the Northwestern Deccan Volcanic Province of India is among the most seismically earthquake-prone. The region may be susceptible to remote dynamic triggering, especially the Kachchh region, which recently hosted the M_w7.7 Bhuj earthquake in 2001. Its aftershocks continue because it is critically stressed and contains nucleation points more frequently close to failure. From waveforms and catalog data, we examine whether remote dynamic triggering occurs following 25 April 2015, M_w7.8 Nepal mainshock in the Gujarat region, Northwestern India. The 2015 Nepal event perturbed the Gujarat region with a peak dynamic stress of ~53 kPa, much higher than the global lower limit of 1 kPa. Due to the large magnitude and high peak dynamic stress, ideally, the 2015 mainshock should have resulted in the triggered seismicity in the study region. To study the remote dynamic triggering in detail, we also have examined the other recent regional large earthquakes with comparable peak dynamic stresses (>50 kPa), namely, 16 April 2013, M_w7.7 Iran, 24 September 2013, M_w7.7 Pakistan, and 26 October 2015, M_w7.7 Afghanistan. Our result shows that despite their significant peak dynamic stress, there is no significant change in the local seismicity. The analysis suggests that the surface wave amplitude is not the only factor that governs the remote dynamic triggering. Our results also indicate that the faults were not critically stressed during the mainshock candidates in the study region.

KEYWORDS

Gujarat region, dynamic stress, remote earthquakes, surface waves, earthquake predication

1 Introduction

April 2015, M_w7.8, Gorkha, Nepal earthquake is one of the disastrous earthquakes which caused widespread damage in Nepal and nearby countries. The earthquake associates itself with a 135 km long rupture length which progressed southeastwards towards its most significant aftershocks (M_w7.3) that occurred after 16 days. It recorded the highest seismic intensity of IX on the MMI scale in the Epicentral region. Prakash et al. (2016) estimated a stress drop of 3.4 MPa for the Nepal earthquake 2015 in the inter-plate region; Han et al. (2017) reported dynamic triggering in southwest China ~2,200 km away during the 2015 Nepal event. Thus, delineating the link between the Nepal event and its triggering capability in Gujarat, NW India, might lead to new insights into dynamic triggering. The Nepal earthquake occurred ~1,200 km away from the Gujarat region (Figure 1A). It is, therefore, important to look for signs of triggering seismicity in the region.

The M_w7.3 Landers earthquake of 1992 (Hill et al., 1993) gave birth to the study of remote triggering. It reinforced the idea of remotely triggered earthquakes; now, the study has matured, but the mechanism of such triggering remains elusive. The magnitude of

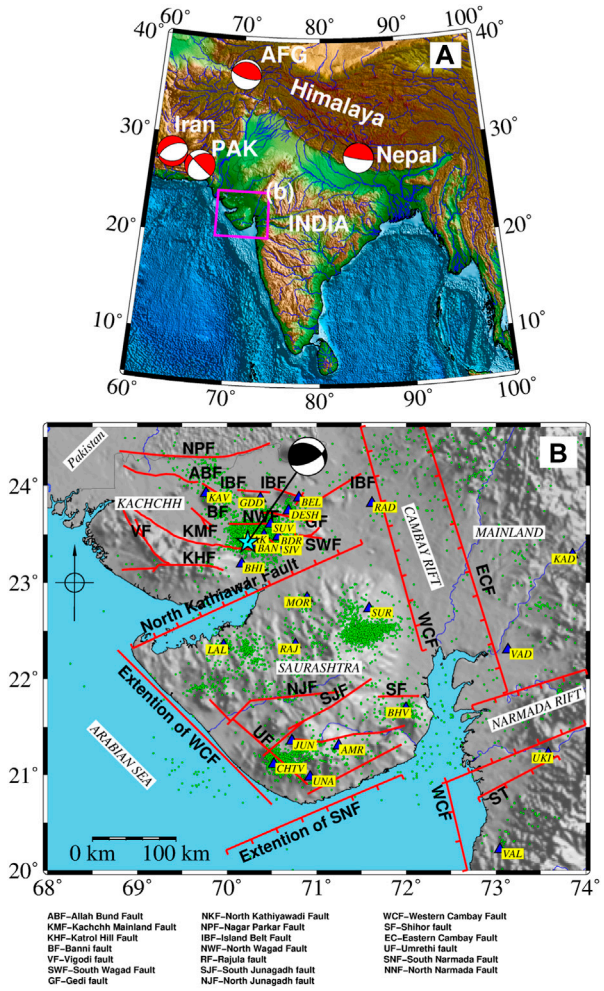

FIGURE 1
(A) Remote mainshocks considered as candidates for the dynamic triggering in the Gujarat region (magenta box), namely, 16 April 2013, M_w7.7 Iran, 24 September 2013, Mw7.7 Pakistan (PAK), 24 April 2015, Mw7.8 Nepal, and 26 October 2015, M_w7.5 Afghanistan (AFG) Earthquakes, along with their focal mechanism. **(B)** Seismotectonic map view of the Gujarat region in Northwestern India. The blue triangles are broadband stations, and the red lines are active faults (Supplementary Table S1), along with the background seismicity since 2007 (green dots). The cyan star is attributed to the 2001 Mw7.7 Bhuj earthquake, and its focal mechanism is also shown.

triggered seismicity is generally less than 2 (Harrington and Brodsky, 2006; Wang et al., 2019), which generally global catalogs miss. Velasco et al. (2008) analyzed 15 earthquakes recorded by 500 globally distributed stations and suggested that remote triggering is ubiquitous. Thus, it is an essential criterion for selecting regions with good-quality earthquake catalogs supplemented with a wide range of digital waveforms to comprehensively study and examine dynamic triggering.

The digital waveform network covers Gujarat, Northwestern India well (Figure 1B). The Kachchh Rift Basin (KRB) is a seismically active intraplate region that also hosted the M_w7.7 Bhuj earthquake in 2001 (Figure 1B). The Bhuj earthquake of 2001 renewed seismologists' interest in understanding the region's geodynamics. The Institute of Seismological Research (ISR) installed the Gujarat Seismic Network (GSNet) in 2006 (Figure 1B). A digital network of 54 accelerographs and 60 high-resolution three-component seismographs has been installed, stretching the entire state of Gujarat. The newer data furnishes an excellent opportunity to interpret the earthquake's origin, and it is undergoing geodynamic processes.

The Northwestern Deccan Volcanic Province, India, has been a host of moderate to major intra-plate earthquakes (Rajendran and Rajendran, 2001; Gupta et al., 2001; Singh et al., 2015). The Bureau of Indian Standards 2002 categorized the KRB in Seismic Zone-V (highly vulnerable). On the other hand, the different regions like Saurashtra Horst (SH) and Mainland (ML) regions of Gujarat are less seismically active than KRB and fall in the seismic zone IV/III. The three physiographical units (SH, ML, and KRB) have different tectonic setups, geology, and seismicity (Biswas, 1987; ISR annual report 2016). The area lies approximately 1,000 km off the region of the Himalayan Collision Zone and about 500 km off the plate boundary of India and Arabian.

In peninsular India, the Kachchh region of Gujarat state, although not located on or near any plate boundary, has been experiencing frequent earthquakes. The KRB evolved during 135 Ma and formed due to extensional tectonics (Kayal et al., 2002a; Kothari et al., 2016). The region is the most active intra-continental region globally, and in addition to the 2001 M_w7.7 Bhuj event, the KRB hosted some of the most significant known intraplate earthquakes, viz, the 1819 Allahbund earthquake (Dam-of-God) (M 7.8), the 1,668 Indus delta (MM X), the 1,845 Lakhpat earthquake (M 6.3, MM VIII), and 1956 Anjar earthquake (M_w6.0) (Gaur, 2001; Rajendran and Rajendran, 2001; Rastogi et al., 2011).

Previous studies have indicated that the formation of the KRB is attributed to rifting along with the E-W tectonic trend. The E-W trending Kachchh region has also been ascertained from the highly abnormal values in the Bouguer gravity data (GSI, 2000; Chandrasekhar and Mishra, 2002). Moreover, the E-W alignment of faults within the basin controls the KRB structurally, the faults being Island Belt Fault (IBF), Banni Fault (BF), Kachchh Mainland Fault (KMF), Katrol Hill Fault (KHF), South Wagad Fault (SWF), North Wagad Fault (NWF) and Gedi Fault (GF) as shown in Figure 1 and described in Supplementary Table S1.

In contrast to the KRB, the SH region of Gujarat is seismically less active. A horst structure bounded by faults on all four edges controls the seismicity in the SH. The SH is bounded by the extended Son Narmada Fault (SNF) and the North Kathiawar Fault (NKF) on the southern edge and its northernmost border, respectively. The West Cambay Fault (WCF) and the WNW–ESE trending West Coast Fault (WCF) are on the eastern edge and the Arabian Sea, respectively. The SH has hosted three medium-sized shallow earthquakes in the Talala region since 2007, M_w4.8 and M_w5.0 in 2007 and M_w5.1 in 2011 (Yadav et al., 2011; Singh et al., 2013; Singh and Mishra, 2015). Historically, the area has also experienced many other earthquakes, such as the M_w6.1 event of 1919 in Bhavnagar, considered the biggest in the region (Rajendran and Rajendran, 2001). Historical earthquakes occur away from plate boundaries and are considered intraplate events. Hence, the stresses therein due to plate boundaries are still unclear.

The ML region of Gujarat is limited by two long boundary fault systems, the Cambay rift basin in the north and the Narmada rift

basin in the south of Gujarat. Further, the Narmada rift is divided into Narmada North Fault (NNF) and the Narmada South Fault (NSF). The most significant event generated by the Narmada lineament is 1970 M_w5.4, with a depth of 10 km and a strike-slip mechanism (Gupta et al., 1972; Chandra, 1977; Rastogi et al., 2012). On the other hand, the NNW-SSE trending Cambay rift basin is seismically less active and bounded to the east by the Great Boundary Fault, and the Aravalli-Delhi Mobile Belt covers the western edge.

Most cases of dynamically triggered events (i.e., unexpected rise in seismicity after large remote earthquakes) are noticed near plate margins or volcanic/geothermal areas (e.g., Peng and Chao, 2008; Aiken and Peng, 2014; Bansal et al., 2016 and reference therein). In the stable regions, remote earthquake triggering was identified in regions with meagre background seismicity rates (Gomberg et al., 2004; Velasco et al., 2008). On the other hand, some studies documented that regions with high background seismicity or regions that have experienced significant earthquakes (or hosted large historical events) in the past are more susceptible to dynamically triggered earthquakes (e.g., Hough et al., 2003; Peng et al., 2010b; Jiang et al., 2010; Dixit et al., 2022a; b), because these regions denote the zones of weakness having several nucleation points (Hill and Prejean, 2007; Savage and Marone, 2008). Hence, the Gujarat region is susceptible to dynamic triggering, and the KRB has a higher chance of being triggerable among SH and ML. The dynamic triggering in other intraplate regions has also been documented (Peng et al., 2010b; Jiang et al., 2010; Wu et al., 2011; Wu et al., 2012; Yao et al., 2015; Bansal et al., 2018; Li et al., 2019).

This article systematically analyzed the local seismicity following the 2015 Nepal event to determine dynamic triggering in the Gujarat region. The ISR catalog has been used to measure the seismicity rate change in the region. 10 Hz high pass waveform data is studied to find micro-earthquakes missing in the ISR catalog. Along with the Nepal earthquake, 2015, we also examined other recent earthquakes having comparable dynamic stresses in the region (i.e., 16 April 2013, M_w7.7 Iran, 24 September 2013, M_w7.7 Pakistan, and 26 October 2015, M_w7.7 Afghanistan Earthquakes (Figure 1A). It is, therefore, helpful to look for triggering due to large earthquakes having comparable dynamic stresses in the region.

2 Data and methodology

The Kachchh Rift Basin, Saurashtra Horst, and the Mainland Gujarat region differ in geology, seismicity, and tectonics, so we selected and separated events in the ISR catalog for the above three regions. The β value quantifies a change in seismicity from the observed seismicity rate before and after the mainshock (Matthews and Rosenberg, 1988; Aron and Hardebeck, 2009).

$$\beta = \frac{N_a - N\left(\frac{T_a}{T}\right)}{\sqrt{\left[N\left(\frac{T_a}{T}\right)\right]\left(1-\frac{T_a}{T}\right)}}$$

Where T_a is the period after the onset of the P wave of the remote mainshock (Triggered Window), T is the total time length of the triggered window plus the background seismicity window (Time window before the arrival of the remote mainshock P wave), N_a is the number of events during the triggered window, and N is the total events during the triggered plus background window. In the study, we used T=48 h and T_a=24 h.

A β≥2 indicates a significant increase in the seismicity, whereas β≤−2 corresponds to a significant decrease in the seismicity (Hill and Prejean, 2015). We computed the β value from the ISR catalog during the 24 h of the main shock. We observed that the β value for the 2015 Nepal event is less than two indicating an insignificant change in the seismicity. A vital portion of triggered events may be missing in the existing catalog because higher amplitude surface waves mask local microearthquakes (Bansal et al., 2018; Dixit et al., 2022a; b). The analyses of continuous waveform data for identifying missing microearthquakes are more viable (e.g., Gomberg et al., 2004; Prejean et al., 2004; Peng et al., 2010a).

Numerous studies examined the waveforms within 1 h after the remote mainshock (e.g., Velasco et al., 2008; Jiang et al., 2010; Li et al., 2019) because most of the seismic activity due to triggering occurred either at the time of the arrival of large surface wave or immediately after it. Hence, we used waveform data in a continuous form recorded by GSNet, 1 h before and after the P-wave of the 2015 Nepal mainshock. Next, we cut the waveforms with surface wave phase velocities between 5 km/s and 2 km/s, covering most of the surface waves, and computed the peak ground velocity (PGV). We measured the Peak Dynamic Stress (PDS) using the relationship $\sigma = \frac{\mu(\mathrm{PGV})}{\upsilon}$, where σ is dynamic stress, υ is the nominal phase velocity (assumed to be 3.5 km s-1), and μ is the shear rigidity (which is assigned a nominal value of 35 GPa) (Aiken and Peng, 2014).

Next, we corrected the raw waveform data of all three components by removing the instrument response. After applying the instrument correction to the raw waveform data, we rotated the north-south and east-west components to a great circle path to obtain the transverse and radial components. Since, the triggered events are generally observed in the high-frequency range, the waveform data is filtered using a 10 Hz high pass filter to confirm possible triggered events. Further, a spectrogram is also generated using a 0.5 Hz high-pass filter using the waveforms containing the vertical component. The GSNet recorded the 2015 Nepal event at 22 stations, eight in the Kachchh, five in the Mainland, and nine in the Saurashtra region. The analyzed raw and 10 Hz high-pass filtered waveforms of the Nepal event recorded at GSNet are shown in Supplementary Figure S1.

3 Results and discussion

We examined the 10 Hz high-pass filtered waveforms and spectrograms at the permanent station in the KRB, SH, and ML regions during the 2015 Nepal event (Figures 2–4). The peak dynamic stresses at the vertical component in the KRB, SH, and ML is greater than 52 kPa. Despite the region's high peak dynamic stresses, we found no evidence of remote triggering during the 2015 Nepal mainshock. However, we identified only one event after the 2015 mainshock at station UNA (Figure 3).

To study the remote dynamic triggering in detail, we have also examined the other recent large earthquakes with comparable peak dynamic stresses (>50 kPa), namely, 16 April 2013, M_w7.7 Iran, 24 September 2013, M_w7.7 Pakistan, and 26 October 2015, M_w7.5 Afghanistan Earthquakes (Supplementary Figure S2–S10).

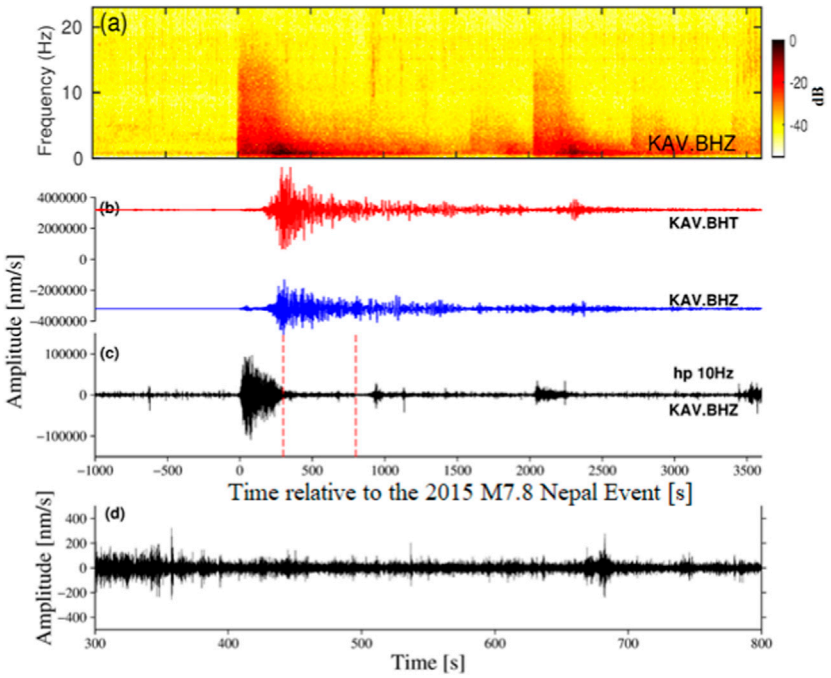

FIGURE 2
Waveform analysis for 25 April 2015, M_w7.8 Nepal mainshock recorded at station KAV in the Kachchh region. **(A)** Spectrogram of the vertical component at KAV station. **(B)** 1 Hz low-pass filtered transverse (red) and vertical (blue) component waveforms were recorded at station KAV. **(C)** 10 Hz high-pass filtered vertical component waveform at station KAV. The portion between two vertical red dotted lines marks the zoom-in window during the surface waves shown in **(D)**.

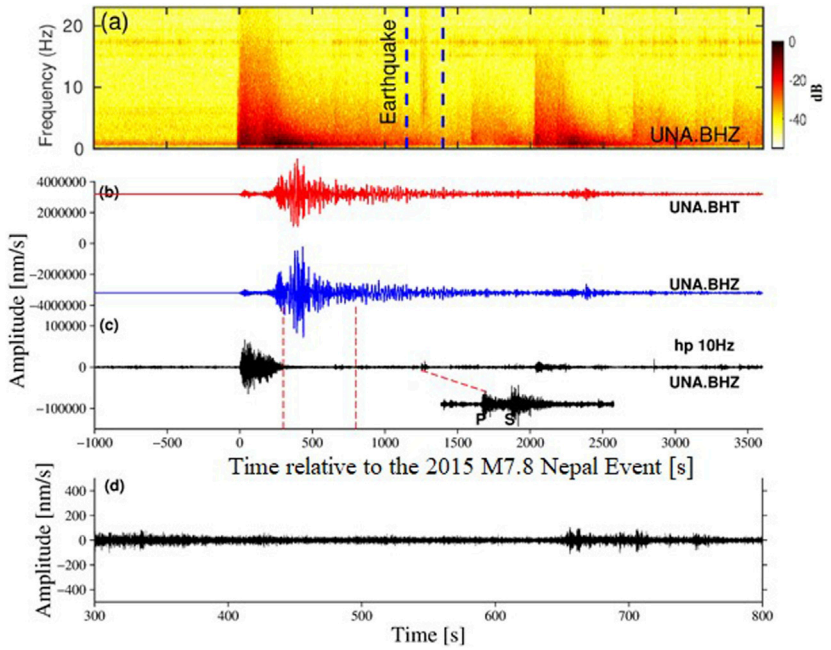

FIGURE 3
Similar plots as Figure 2 during 25 April 2015, M_w7.8 Nepal mainshock recorded at station UNA in the Saurashtra region.

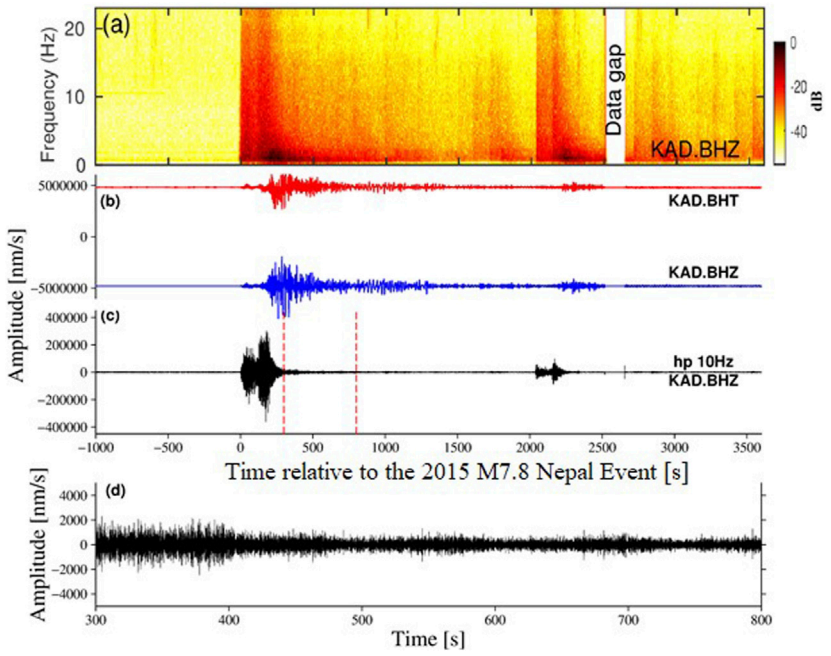

FIGURE 4
Similar plots as Figure 2 during 25 April 2015, M_w7.8 Nepal mainshock recorded at station KAD in the Mainland region.

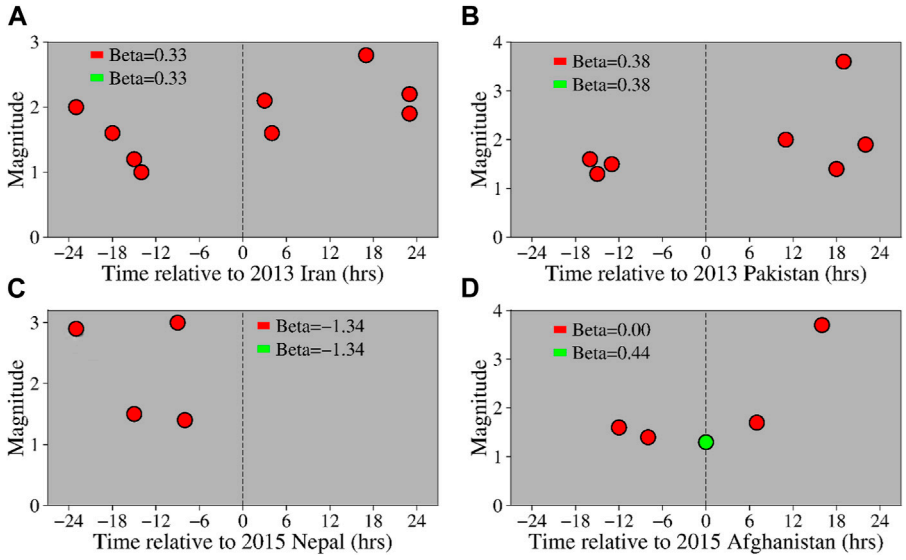

FIGURE 5
Seismicity changes in the Kachchh region 24 h before and after the four regional candidates were considered for the study. Red circles are events listed in the ISR catalog, whereas green circles are manually identified events. The vertical dotted black line is the main event. The β value uses only catalog events, and all events (catalog+identified manually) are also shown in the red and green color bars, respectively.

We followed the same procedure as the 2015 Nepal event. We found that there is an indication of an increase in seismicity during 2013 Pakistan (Supplementary Figure S6) and the 2015 Afghanistan (Supplementary Figure S8,S10). However, as in the case of the 2015 Nepal event, we found only one or two earthquakes just after the surface waves of the 2013 Pakistan and 2015 Afghanistan earthquakes. Notably, these identified microearthquakes are not listed in the ISR catalog. To check the seismicity increase, we added these identified events to the ISR catalog (green circles in Figures 5–7) and calculated the β values again. In addition to manually picking local events, we identified local peaks using STA/LTA (Short-term algorithm/Long-term

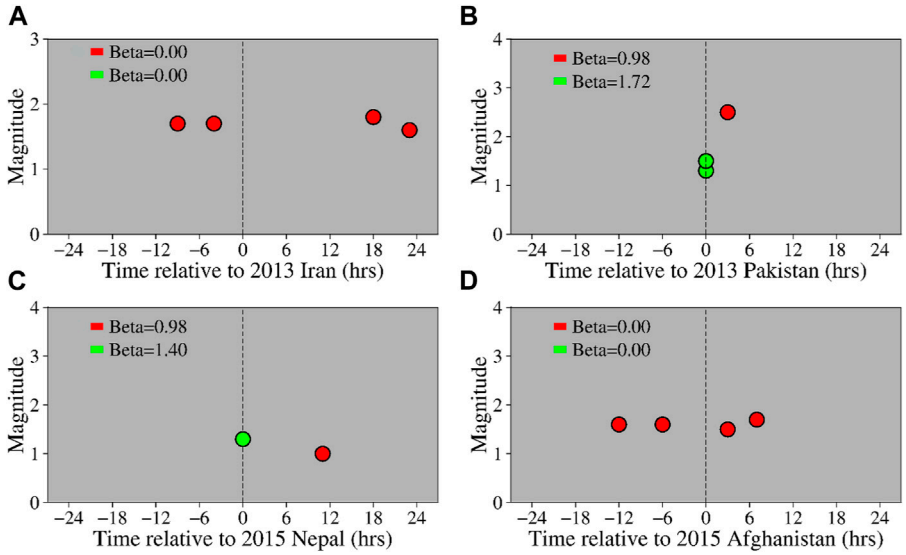

FIGURE 6
Same as Figure 5, but for the Saurashtra region.

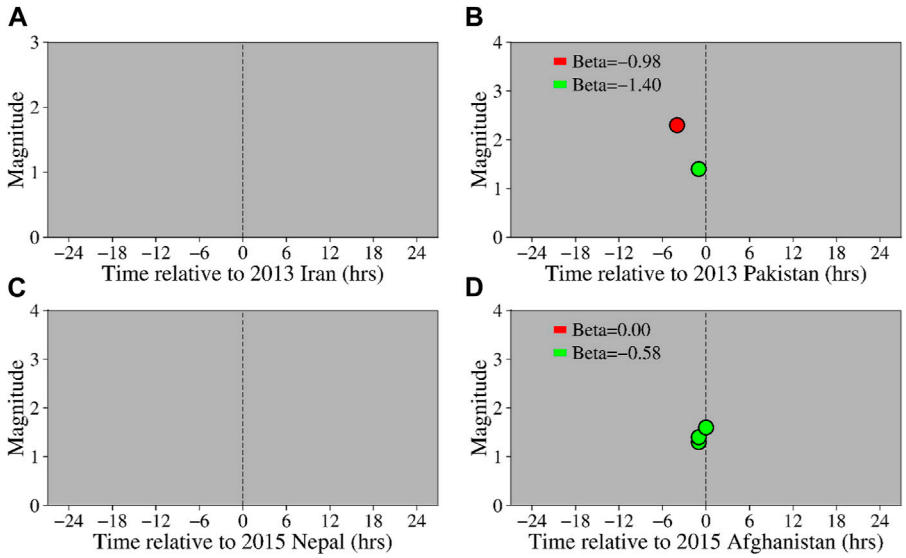

FIGURE 7
Same as Figure 5, but for the Mainland region.

algorithm) and then calculated the β. We found that the β value is less than 2 for all four mainshocks at all the stations, suggesting that the triggering is not statistically significant (Figures 5–7, Supplementary Figure S11,S12).

3.1 Factors affecting dynamic triggering

Recent observations from field data and laboratories suggested that amplitude and frequency (e.g., Gomberg and Davis, 1996; Brodsky and Prejean, 2005; Gomberg and Johnson, 2005; Johnson and Jia, 2005; Hill and Prejean, 2007), mainshock rupture propagation direction (Jiang et al., 2010; Li et al., 2019), direction of incoming waves (Chao et al., 2012; Bansal and Ghods, 2021) play a significant role in causing dynamically triggered earthquakes. Dixit et al. (2022b) shown that a combination of parallel incidence and local stress conditions are the factors that control the apparent triggering threshold in the Kachchh region. Moreover, Chao et al. (2012) found that amplitude, intermediate/long-period surface waves, and incidence angle govern the triggering

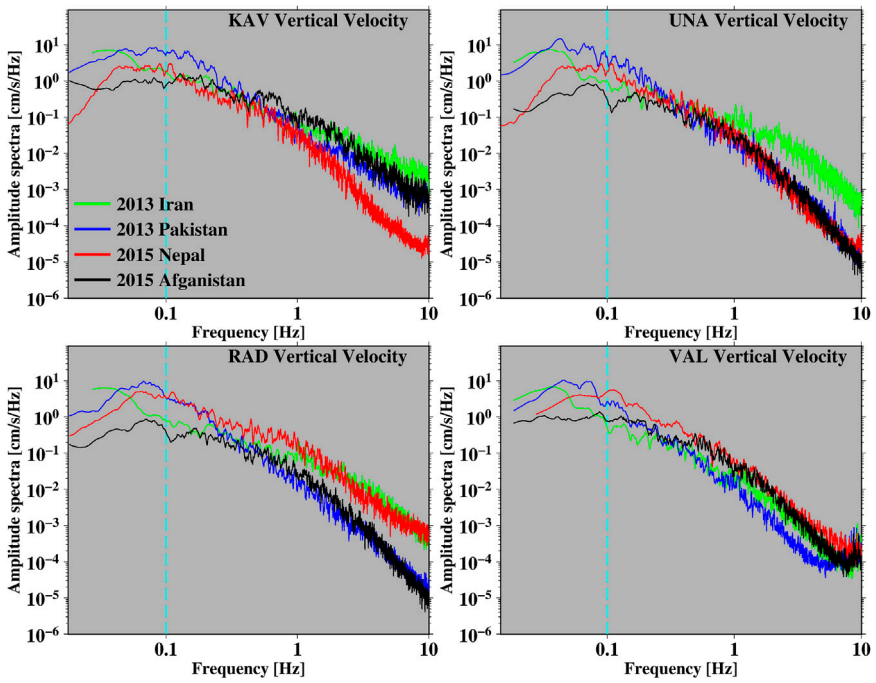

FIGURE 8
Comparison of velocity spectra of the vertical component of the four regional events in the Kachchh (KAV), Saurashtra (UNA), and Mainland (RAD and VAL) of Gujarat region. The vertical dashed cyan line is the mark of 10 s.

around Taiwan. Furthermore, Naves et al. (2018) also suggested that tectonic regimes cannot solely explain remote dynamic triggering mechanisms.

Dixit et al. (2022a) have shown that the high dynamic stresses, low frequency of surface waves of the 2012 Indian Ocean mainshock, and background seismicity in the Mainland region of Gujarat, India, are responsible for triggering. It is also noted that triggered seismic activity is more preferably caused due to the energy released by low-frequency waves rather than the waves with high frequency within the same amplitude range in California's Long Valley Caldera region (Brodsky and Prejean, 2005). Savage and Marone (2008), through their laboratory studies, also suggested that amplitude, frequency of the input motion, and the state of stresses within the faults are the prime factors governing earthquake triggering in a region. Additionally, dynamically triggered earthquakes are more likely to occur when a fault is about to fail (Rubinstein et al., 2009). However, the underlying nucleation mechanisms and the dominant phenomenon are still elusive (Mendoza et al., 2016).

3.1.1 Triggering as a function of amplitude

Recent researchers have presented that the dynamic stress of the incoming surface waves might be one of the reasons behind the dynamic triggering of earthquakes (Brodsky and Prejean, 2005; Peng et. al., 2009; Aiken et. al., 2013). The 2013 Pakistan earthquake generated the highest peak dynamic stresses (53.37 kPa, Supplementary Table S2) among the analyzed mainshocks. However, the other three events also caused peak dynamic stress above 50 kPa (Supplementary Table S2). Despite their high peak dynamic stresses, these events also did not significantly increase seismicity (Figures 5–7).

Han et al. (2017) performed surface wave modelling of the 2015 Nepal mainshock and showed that the triggering occurred during the first two cycles of the Rayleigh waves. Similarly, we have modelled the surface wave propagation to understand the relationship between the triggered events and the triggering waveform. We found no events during the dilatational stress similar to the study of Han et al. (2017) (Supplementary Figure S13), suggesting that peak dynamic stresses are not the only criteria for remote triggering. Recently, Bansal and Ghods (2021) have proposed that the amplitude of the dynamic stresses is not an adequate criterion. Dixit et al. (2022b) have also shown that the 2010 Chile, 2011 Tohoku-Oki, and 2012 Indian Ocean earthquakes did not trigger any seismicity in the Kachchh region of Gujarat despite their significant dynamic stresses. Our results are consistent with earlier studies and suggest that the peak dynamic stress is not the only factor that controls the remote dynamic triggering.

3.1.2 Triggering as a function of frequency

In this section, we quantify the triggering as a function of input frequency by computing the amplitude spectra of surface waves for all four mainshocks. We first cut the instrument-corrected velocity seismograms within the apparent velocity of 5–2 km/s to include most of the surface waves. Next, we compute the corresponding spectra for the vertical component and smooth the resulting spectra with a sliding window of 10 points. Figure 8 shows the vertical components' velocity spectra at KAV, UNA, RAD, and VAL stations for the four mainshocks.

Peng et al. (2009) shown that the surface wave energy is most prominent between 10 to 100 s, especially in the range of 20–60 s, for the study of tremors along the San Andreas Fault in central

California. Furthermore, the 2002 Denali Fault and 2003 Colima earthquakes, which generated the highest spectra in the frequency range of 10 to 1 s, also triggered the tremors around Parkfield. Bansal et al. (2018) found low-frequency (period 10–33 s) surface waves from the 2012 M_w8.6 Indian Ocean earthquake triggered seismicity in the Koyna-Warna intraplate region. Recent studies shown that low-frequency surface waves (longer than 10 s) are more efficient in triggering seismicity (Brodsky and Prejean, 2005; Guilhem et al., 2010; Chao et al., 2012; Dixit et al., 2022a). Seismic energy between 10 to 100 s determines whether an earthquake can trigger seismicity. In our case, the 2013 Pakistan event generated the highest spectra among the mainshocks (Figure 8) in a low-frequency range. However, it is noteworthy that none of the mainshocks dominated the above-described frequency ranges. Hence, these events cannot generate the significant low-frequency energy that can trigger seismicity.

3.2 Background seismicity

As mentioned, Gujarat's three tectonically active blocks belong to the stable continental region in the western part of peninsular India. The KRB, the most seismically active region, recently hosted the 2001 M_w7.7 Bhuj earthquake, and the aftershock activity continues (Rastogi et al., 2012). On the other hand, the SH and ML are not as active as KRB and fall in the seismic zone IV/III (BIS, 2002). The Cambay and Narmada rifts of the ML are hitherto considered as a stable continental region that is seismically less active. Only ~800 earthquakes occurred between 2006 and 2017, corresponding to 0.2 quakes per day (recorded by GSNet). Since 2007, the average daily number of earthquakes (M≥1) in KRB, SH, and ML are 3.1, 1.9, and 0.2, respectively.

Recent studies reveal that dynamic triggering by distant earthquakes is more likely in the active plate margin areas or in the regions experiencing aftershocks of large earthquakes (e.g., Hill et al., 1993; Hough et al., 2003; Jiang et al., 2010). Hence, KRB, which hosted the M_w7.7 earthquake in 2001, maybe the most triggerable among SH and ML. In this section, we will apply the two proposed mechanisms for long-range triggering, i.e., the subcritical crack growth model (Brodsky et al., 2000; Gomberg et al., 2001) and unclogging of fractures via crustal fluid (Brodsky et al., 2003).

Dieterich (1994) postulates that following a perturbation, R, the seismicity rate is directly proportional to 'r', which is the seismicity in steady-state.

$$R = r \exp\left(\frac{\Delta\tau}{A\sigma}\right)$$

Where constant A and σ are material properties and normal stress, respectively (Dieterich 1994).

Suppose we assume the above equation, given high background seismicity. In that case, the rate of seismicity change is expected to be quite higher following perturbations due to remote mainshocks, contrary to what we observed. Faults or a group of faults, when are about to experience failure, transient stresses caused by surface waves can activate critically stressed faults. A critically stressed fault gets perturbed by any change in small stresses that can give rise to brittle failure (Gomberg et al., 1998). The model relating to the subcritical crack growth draws attention to the idea that the amount of stresses accumulated at the crack tip concerning the crack size governs the further crack growth rate or, more commonly, the earthquake nucleation (Atkinson, 1984). Initially, the crack grows very slowly and then rapidly, leading to delayed fault rupture upon an unexpected rise in stresses at the crack tip (Atkinson, 1984; Rinne, 2008). Therefore, if the background seismicity rate and undergoing stresses are comparable and follow the subcritical crack growth model in Gujarat, then there should be significant dynamic triggering in the region.

In the KRB, magnetotelluric and 3-D local earthquake tomography suggested fluids at the shallow brittle-ductile boundary in the epicentral zone of the 2001 Bhuj earthquake (Kumar et al., 2017). The oscillatory stresses (Li et al., 2019) started by remote mainshocks could enhance the fluid permeability, decreasing the rock strength by lessening the effective normal stresses across preexisting faults. When the high amplitude surface waves interact with fluids in the crust, they can promote new micro-cracks, new crustal-scale shear zones, and unclogging fractures (Tullis et al., 1996; Hardebeck and Hauksson, 1999; Cox, 2002; Brodsky et al., 2003). The stresses increase pore pressure (Hill et al., 1993; Brodsky and van der Elst, 2014; Li et al., 2019), making the region more susceptible to dynamic triggering. Shaking activity that lasts longer persistently agitates the crustal fluid, thus resulting in triggered seismicity. Since analyzed mainshocks are near the study area, the surface waves are generated for a short interval.

It has been noticed in Figure 9 for the Kachchh region that 10 days before mainshocks, the total number of average earthquakes is greater than the average number of earthquakes since 2007 (except for the 2015 Nepal event), thus attaining high background seismicity levels before the remote earthquakes took place. So earthquake activity before the mainshocks indicates the liberation of accumulated stress, and the near-critical state required for remote triggering in the study region was missing (Peng et al., 2009). Such loss of stored stress before the events is likely responsible for the non-triggering of microearthquakes in the study area despite their high peak dynamic stresses. In the case of the 2015 Nepal event, we found no noticeable seismicity rate changes (Figures 2–7), suggesting that the faults during the 2015 Nepal event were not critically stressed. A similar pattern of high background seismicity is found in the SH region (except for 2013, Iran, and Pakistan, Figure 10). As mentioned above, the seismicity in the ML region is very low, and we found few earthquakes before the mainshocks (Figure 11).

3.3 Mainshock rupture propagation direction

Some recent studies have shown that the direction of rupture propagation could also cause the triggering of seismicity. Jiang et al. (2010) found that triggering is most prominent in the rupture propagation direction of the M_w7.9 Wenchuan earthquake of 2008. Additionally, Li et al. (2019) showed that the rupture direction of the 2004 M_w9.1 Sumatra earthquake was almost

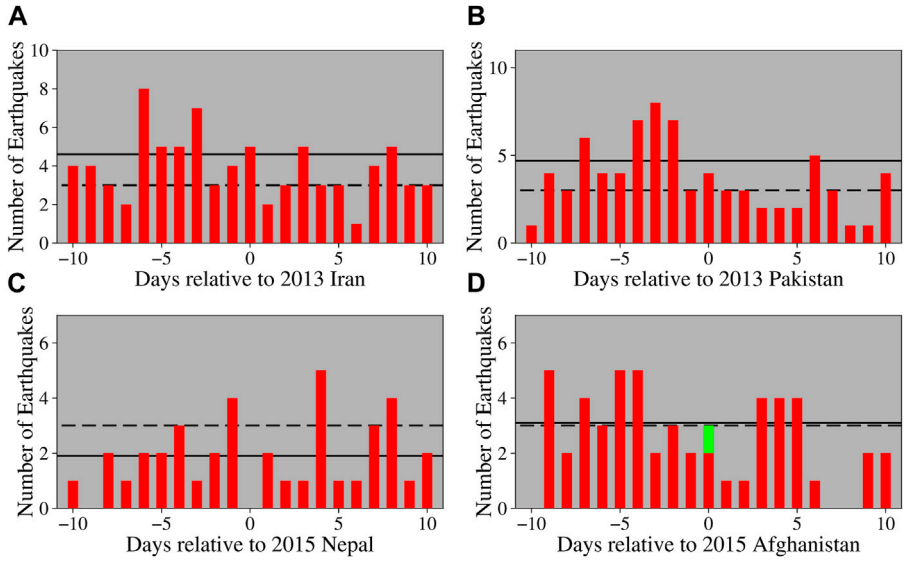

FIGURE 9
Seismicity changes in the Kachchh region 10 days before and after the four candidates considered for the study. Red bars are events listed in the ISR catalog, whereas green bars are events identified manually. The horizontal dotted and solid black lines are the average number of earthquakes since 2007 and 10 days before the mainshock, respectively.

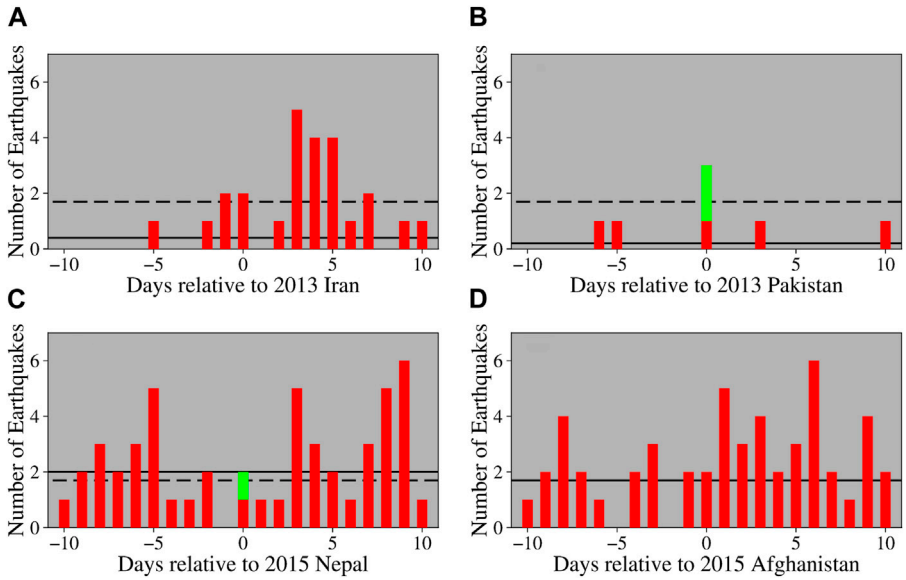

FIGURE 10
Same as Figure 9, but for the Saurashtra region.

directly towards the Yunnan, SW China. Fan and Shearer (2015) showed that the rupture of the 2015 Nepal mainshock propagated for ~160 km at an azimuth of ~130° with an average rupture velocity of 2.9 km/s, which is not towards the Gujarat region. Additionally, the other three mainshocks' rupture direction was not towards the Gujarat region (Figure 12). The rupture direction may be one of the possible causes for triggering in a region.

3.4 Tectonic regime

GPS studies have shown that the KRB is experiencing a north-south compression rate of ~4–5 mm/year, which makes it highly seismically active (Gahalaut et al., 2019). Additionally, Singh et al. (2016) have shown that most faults are either thrust or reverse faults with the strike-slip mechanism. Anderson's theory suggests that the

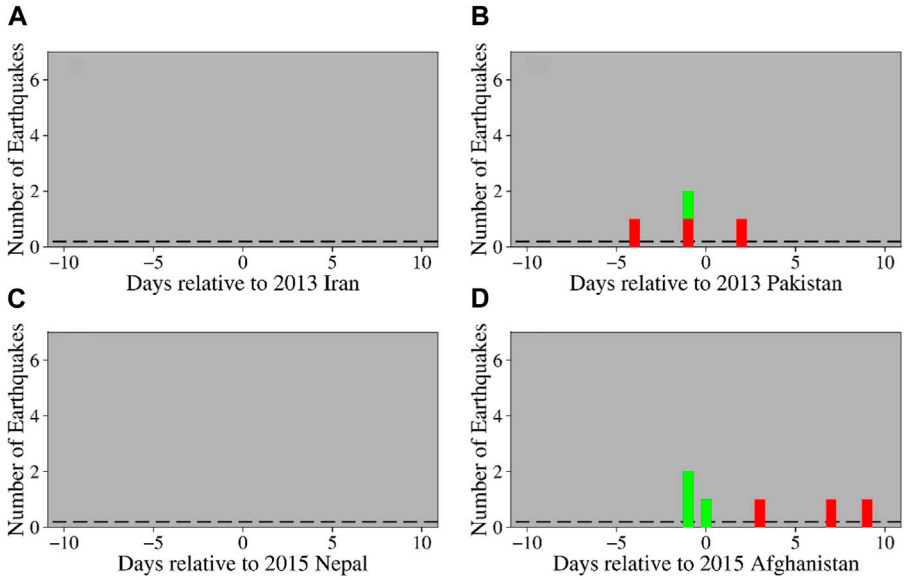

FIGURE 11
Same as Figure 9, but for the Mainland region.

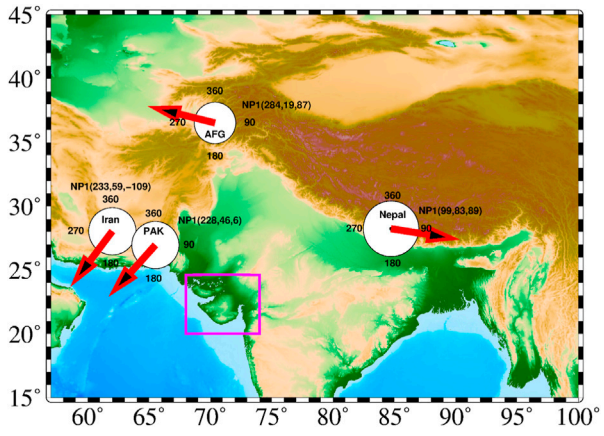

FIGURE 12
Rupture propagation direction (red arrow) of the four regional candidates considered for the study (magenta box). The nodal plains (NP1, strike, dip rake) is taken from the earthquake. usgs.gov/earthquakes/eventpage.

horizontality of the principle of comprehensive stress results in a higher amount of gross stress; hence, a higher degree of differential stress is required for thrust faults to rupture (Sibson, 1974). Also, if only the stress regimes are considered, areas comprising weaker faults in localized extension tend to experience remote dynamic triggering more easily. However, this idea is still debatable as tectonic settings with extensional and trans-extensional features have yet to be examined (Aiken et al., 2013). Nevertheless, the influence of dynamic perturbation over the earthquake cycle related to faults is still under debate (Mendoza et al., 2016). Harrington and Brodsky (2006) showed a lack of remotely triggered seismicity in the compressional tectonic environment. Hence, the tectonic setting is an essential factor for the remote triggering in a region.

3.5 Direction of incoming waves

The Gujarat region was dominated by thrust, strike-slip, or mixed-type (thrust and strike-slip) earthquakes. In the Kachchh region, the historical earthquakes of M>4.0 are mixed types (Singh et al., 2016). Additionally, in the Saurashtra region, all the events of M>4.0 are strike-slip (Yadav et al., 2011), and the 1971 M5.4 Bharuch earthquake in the Narmada rift zone of the Mainland region is also a strike-slip with thrust component (Gupta et al., 1972; Chandra, 1977). As mentioned previously, the Kachchh region recently hosted the 2001 M_w7.7 Bhuj earthquake, so the aftershock zone of the 2001 Bhuj earthquake acts as a weak zone with several nucleation points and is more frequently prone to failure (Hill and Prejean, 2007; Savage and Marone, 2008), and has a higher chance to be triggerable among SH and ML. In this section, we will attempt to quantify a relationship between the direction of incoming waves from remote mainshocks and fault orientation in the Gujarat region, especially in the Kachchh region.

Previous studies have shown that strike-parallel incidence of the incoming surface waves relative to the faults is significant (e.g., Chao et al., 2012; Aiken et al., 2013). Bansal and Ghods. (2021) showed that the incidence angle of the triggering surface waves is parallel to the strike of the NE Iran faults. Alfaro-Diaz et al. (2020) also observed the same phenomenon in Coso geothermal region. Anderson's theory suggests that σ_1 (maximum horizontal stress axis) is the largest for thrust and strike-slip faults, and vertical stress (σ_3) is the most significant principal stress for normal faults. As mentioned earlier, the Kachchh region has faults of EW trending planes (Figure 1B and Supplementary Figure S14), most of which are

either thrust/reverse, strike-slip, or mixed type (thrust and strike-slip), implying that the σ_1 is dominant in the Kachchh region. In addition to the background static stress loading, additional dynamic stress is provided in the direction of the σ_1. i.e., in that case, the waves which are incident on the EW trending faults in the direction of σ_1 will be more triggerable. In the study, the waves from the remote candidates are not incident parallel to the EW trending faults (Supplementary Figure S14,S15) and thus have less chance for triggering. In the case of Normal faulting (which is absent in the study region), they will have a higher chance of triggering because, in that case, the waves will hit the faults in the direction of σ_3.

4 Conclusion

The study suggested remote dynamic triggering does not occur in the Gujarat region following the 2015 Nepal earthquake. Similarly, with their significant peak dynamic stress, other large earthquakes did not trigger seismicity. The research finding suggests that the surface wave amplitude is not the only factor that controls the remote dynamic triggering. The rupture direction and orientation of faults with incoming surface waves may play an essential role. The following factors, either individually or in combination, may be responsible for dynamic triggering: 1) The region should be critically stressed, 2) significant low-frequency surface waves, 3) rupture propagation direction of the mainshocks, 4) compressional tectonic regime, and 5) direction of incoming waves from remote mainshocks.

Data and resources

The waveform and catalog data used in the study have been obtained from the Seismic Data Analysis Center, Institute of Seismological Research (ISR), Gandhinagar, Gujarat. The data can be obtained by requesting the Director-General, ISR. The Seismic Analysis Code (Goldstein et al., 2003) and SEISAN (https://www.geo.uib.no/seismo/SOFTWARE/SEISAN/) are used to process data. All figures were made using either Generic Mapping Tools (Wessel et al., 2013) or MATLAB. The Supplementary Material for this article includes 2 tables and 15 figures.

Data availability statement

The data analyzed in this study is subject to the following licenses/restrictions. The waveform and catalog data used in the study have been obtained from Seismic Data Analysis Center, Institute of Seismological Research (ISR), Gandhinagar, Gujarat. The data obtained from a running project supported by the Department of Science and Technology, Government of Gujarat, India. The data can be obtained by requesting the Director-General, ISR. Requests to access these datasets should be directed to The Director General, dg-isr@gujarat.gov.in, director.isr@gmail.com.

Author contributions

MD: Conceptualization, Methodology, Original draft preparation; AB: Supervision, Reviewing and Editing of Manuscript, Overall Guidance. All authors contributed to the article and approved the submitted version.

Funding

AB is supported by the CSIR-NGRI main lab project (MLP-6405).

Acknowledgments

We thank the Director-General of ISR for all his invaluable support and permission to conduct this research. AB thanks the Director, NGRI, for permitting the paper's publication. MD thanks S. Prizomwala, G. C. Kothyari and Rakesh Prajapat for their valuable discussions during the study. ARB is supported by the CSIR-NGRI main lab project (MLP 6405). The ISR operates and maintains the GSNet under a project supported by the Department of Science and Technology, Government of Gujarat.

Conflict of interest

The authors declare that the research was conducted in the absence of any commercial or financial relationships that could be construed as a potential conflict of interest.

Publisher's note

Supplementary material

The Supplementary Material for this article can be found online at: https://www.frontiersin.org/articles/10.3389/feart.2023.1062916/full#supplementary-material

References

Aiken, C., Peng, Z., and Chao, K. (2013). Tremors along the Queen Charlotte Margin triggered by large teleseismic earthquakes. *Geophys. Res. Lett.* 40, 829–834. doi:10.1002/grl.50220

Aiken, C., and Peng, Z. (2014). Dynamic triggering of microearthquakes in three geothermal/volcanic regions of California. *J. Geophys. Res. Solid Earth* 119, 6992–7009. doi:10.1002/2014jb011218

Alfaro-Diaz, R., Velasco, A. A., Pankow, K., and Kilb, D. (2020). Optimally oriented remote triggering in the Coso geothermal region. *J. Geophys. Res. Solid Earth* 125, 1. doi:10.1029/2019JB019131

Aron, A., and Hardebeck, J. L. (2009). Seismicity rate changes along the central California coast due to stress changes from the 2003 M 6.5 San Simeon and 2004 M 6.0 Parkfield earthquakes. *Bull. Seismol. Soc. Am.* 99 (4), 2280–2292. doi:10.1785/0120080239

Atkinson, B. K. (1984). Subcritical crack growth in geological materials. *J. Geophys. Res. Solid Earth* 89 (B6), 4077–4114. doi:10.1029/JB089iB06p04077

Bansal, A. R., and Ghods, A. (2021). Remote triggering in Iran: Large peak dynamic stress is not the main driver of triggering. *Geophys. J. Int.* 225 (1), 456–476. doi:10.1093/gji/ggaa573

Bansal, A. R., Rao, N. P., Peng, Z., Shashidhar, D., and Meng, X. (2018). Remote triggering in the Koyna-Warna reservoir-induced seismic zone, Western India. *J. Geophys. Res. Solid Earth* 123, 2318–2331. doi:10.1002/2017JB014563

Bansal, A. R., Yao, D., Peng, Z., and Sianipar, D. (2016). Isolated regions of remote triggering in south/southeast asia following the 2012 M_w 8.6 Indian Ocean earthquake: Triggered seismicity in southeast asia, *Geophys. Res. Lett.*, 43, 10,654–10,662. doi:10.1002/2016GL069955

Biswas, S. K. (1987). Regional tectonic framework, structure and evolution of the Western marginal basins of India. *Tectonophysics* 135, 307–327. doi:10.1016/0040-1951(87)90115-6

Brodsky, E. E., Karakostas, V., and Kanamori, H. (2000). A new observation of dynamically triggered regional seismicity: Earthquakes in Greece following the August 1999 Izmit, Turkey earthquake. *Geophys. Res. Lett.* 27, 2741–2744. doi:10.1029/2000gl011534

Brodsky, E. E., and Prejean, S. G. (2005). New constraints on mechanisms of remotely triggered seismicity at Long Valley Caldera. *J. Geophys. Res. Solid Earth* 110, B04302. doi:10.1029/2004JB003211

Brodsky, E. E., Roeloffs, E., Woodcock, D., Gall, I., and Manga, M. (2003). A mechanism for sustained groundwater pressure changes induced by distant earthquakes. *J. Geophys. Res. Solid Earth* 108 (B8), 2390. doi:10.1029/2002JB002321

Brodsky, E. E., and van der Elst, N. J. (2014). The uses of dynamic earthquake triggering. *Ann. Rev. Earth planet. Sci.* 42, 317–339. doi:10.1146/annurev-earth-060313-054648

Bureau of Indian Standards (BIS) (2002). *IS 1893 (Part 1)-2002: Indian standard criteria for earthquake resistant design of structures: Part 1 - general provisions and buildings*. New Delhi, India: Bureau of Indian Standards.

Chandra, U. (1977). Earthquakes of peninsular India—a seismotectonic study. *Bull. Seismol. Soc. Am.* 67 (5), 1387–1413. doi:10.1785/BSSA0670051387

Chandrasekhar, D. V., and Mishra, D. C. (2002). Some geodynamic aspect of Kachchh basin and seismicity: An insight from gravity studies. *Curr. Sci.* 83, 492–498. Available at: www.jstor.org/stable/24106853.

Chao, K., Peng, Z., Wu, C., Tang, C. C., and Lin, C. H. (2012). Remote triggering of nonvolcanic tremor around Taiwan. *Geophys. J. Int.* 188, 301–324. doi:10.1111/j.1365-246x.2011.05261.x

Cox, S. (2002). Fluid flow in mid-to deep crustal shear systems: Experimental constraints, observations on exhumed high fluid flux shear systems, and implications for seismogenic processes. *Earth Planets Space* 54, 1121–1125. doi:10.1186/BF03353312

Dieterich, J. (1994). A constitutive law for rate of earthquake production and its application to earthquake clustering. *J. Geophys. Res. Solid Earth* 99, 2601–2618. doi:10.1029/93jb02581

Dixit, M., Bansal, A. R., Kumar, M. R., Kumar, S., and Teotia, S. S. (2022b). The sensitivity of the intraplate Kachchh Rift Basin, NW India to the direction of incoming seismic waves of teleseismic earthquakes. *Geophys. J. Int.* 232, 17–36. doi:10.1093/gji/ggac289

Dixit, M., Bansal, A. R., Kumar, M. R., Roy, K. S., and Teotia, S. S. (2022a). Dynamically triggered events in a low seismically active region of Gujarat, northwest India, during the 2012 Mw 8.6 Indian Ocean earthquake. *Bull. Seismol. Soc. Am.* XX, 1–13. doi:10.1785/0120210142

Fan, W., and Shearer, P. M. (2015). Detailed rupture imaging of the 25 April 2015 Nepal earthquake using teleseismicPwaves: Rupture of the 2015 Nepal earthquake. *Geophys. Res. Lett.* 42 (14), 5744–5752. doi:10.1002/2015GL064587

Gahalaut, V. K., Gahalaut, K., Dumka, R. K., Chaudhury, P., and Yadav, R. K. (2019). Geodetic evidence of high compression across seismically active Kachchh paleorift, India. *Tectonics* 38 (8), 3097–3107. doi:10.1029/2019TC005496

Gaur, V. K. (2001). The rann of Kachchh earthquake. *January 26 2001 Curr. Sci.* 80, 338–340. Available at: www.jstor.org/stable/24105692.

Goldstein, P., Dodge, D., Firpo, M., and Minner, L. (2003). "SAC2000: Signal processing and analysis tools for seismologists and engineers," in *Invited contribution to the IASPEI international handbook of earthquake and engineering seismology*. Editors W. H. K. Lee, H. Kanamori, P. C. Jennings, and C. Kisslinger (London, United Kingdom: Academic Press), 1613–1614. doi:10.1016/S0074-6142(03)80284-X

Gomberg, J., Beeler, N. M., Blanpied, M. L., and Bodin, P. (1998). Earthquake triggering by transient and static deformations. *J. Geophys. Res. Solid Earth* 103 (B10), 24411. doi:10.1029/98JB01125

Gomberg, J., Bodin, P., Larson, K., and Dragert, H. (2004). Earthquake nucleation by transient deformations caused by the M = 7.9 Denali, Alaska, earthquake. *Nature* 427, 621–624. doi:10.1038/nature02335

Gomberg, J., and Davis, S. (1996). Stress-strain changes and triggered seismicity at the Geysers, California. *J. Geophys. Res. Solid Earth* 101 (B1), 733–749. doi:10.1029/95jb03250

Gomberg, J., and Johnson, P. A. (2005). Dynamic triggering of earthquakes. *Nature* 437, 830. doi:10.1038/437830a

Gomberg, J., Reasenberg, P. A., Bodin, P. L., and Harris, R. A. (2001). Earthquake triggering by seismic waves following the Landers and Hector Mine earthquakes. *Nature* 411 (6836), 462–466. doi:10.1038/35078053

GSI (2000). *Seismotectonic atlas of India and its environs*. Kolkata: Geological Survey of India, Special Publication Number 59.

Guilhem, A., Peng, Z., and Nadeau, R. M. (2010). High-frequency identification of non-volcanic tremor along the San Andreas Fault triggered by regional earthquakes, *Geophys. Res. Lett.*, 37, L16309. doi:10.1029/2010GL044660

gujarat, Available at: isr.gujarat.gov.in/sites/default/files/annual-report-2016-17.pdf.

Gupta, H. K., Mohan, I., and Narain, H. (1972). The broach earthquake of march 23, 1970. *Bull. Seismol. Soc. Am.* 62, 47–61. doi:10.1785/bssa0620010047

Gupta, H. K., Rao, N. P., Rastogi, B. K., and Sarkar, D. (2001). The deadliest intraplate earthquake. *Science* 291, 2101–2102. doi:10.1126/science.1060197

Han, L., Peng, Z., Johnson, C. W., Pollitz, F. F., Li, L., Wang, B., et al. (2017). Shallow microearthquakes near Chongqing, China triggered by the Rayleigh waves of the 2015 M7.8 Gorkha, Nepal earthquake. *Earth Planets Sci. Lett.* 479, 231–240. doi:10.1016/j.epsl.2017.09.024

Hardebeck, J. L., and Hauksson, E. (1999). Role of fluids in faulting inferred from stress field signatures. *Science* 285, 236–239. doi:10.1126/science.285.5425.236

Harrington, R. M., and Brodsky, E. E. (2006). The absence of remotely triggered seismicity in Japan. *Bull. Seismol. Soc. Am.* 96, 871–878. doi:10.1785/0120050076

Hill, D. P., and Prejean, S. (2015). Dynamic triggering, in *V. 4 earthquake seismology, treatise on Geophysics*, 2nd (G. Schubert, ed. in *chief) edited by H. Kanamori*Elsevier, Oxford. doi:10.1016/B978-0-444-53802-4.00078-6

Hill, D. P., and Prejean, S. G. (2007). "Dynamic triggering," in *Earthquake seismology treatise on Geophysics*. Editor H. Kanamori (Amsterdam: Elsevier). doi:10.1016/B978-044452748-6.00070-5

Hill, D. P., Reasenberg, P. A., Michael, A., Arabaz, W. J., Beroza, G., Brumbaugh, D., et al. (1993). Seismicity remotely triggered by the magnitude 7.3 Landers, California, earthquake. *Science* 260 (5114), 1617–1623. doi:10.1126/science.260.5114.1617

Hough, S. E., Seeber, L., and Armbruster, J. G. (2003). Intraplate triggered earthquakes: Observations and interpretation. *Bull. Seismol. Soc. Am.* 93, 2212–2221. doi:10.1785/0120020055

Jiang, T., Peng, Z., Wang, W., and Chen, Q. F. (2010). Remotely triggered seismicity in continental China following the 2008 Mw 7.9 wenchuan earthquake. *Bull. Seismol. Soc. Am.* 100 (5B), 2574–2589. doi:10.1785/0120090286

Johnson, P. A., and Jia, X. (2005). Nonlinear dynamics, granular media, and dynamic earthquake triggering. *Nature* 437, 871–874. doi:10.1038/nature04015

Kayal, J. R., De, R., Ram, S., Srirama, B. V., and Gaonkar, S. G. (2002a). Aftershocks of the January 26, 2001 Bhuj earthquake in Western India and its seismotectonic implications. *J. Geogical Soc. India* 59, 395–417.

Kothyari, G. C., Rastogi, B. K., Morthekai, P. B., Dumka, R. K., and Kandregula, R. S. (2016). Active segmentation assessment of the tectonically active South Wagad Fault in Kachchh, western peninsular India. *Geomorphology* 253, 491–507. doi:10.1016/j.geomorph.2015.10.029

Kumar, G. P., Mahesh, P., Nagar, M., Mahender, E., Kumar, V., Mohan, K., et al. (2017). Role of deep crustal fluids in the Genesis of intraplate earthquakes in the Kachchh region, northwestern, India. *Geophys. Res. Lett.* 44, 4054–4063. doi:10.1002/2017GL072936

Li, L., Wang, B., Peng, Z., and Li, D. (2019). Dynamic triggering of microseis-micity in Southwest China following the 2004 Sumatra and 2012 Indian Ocean earthquakes. *J. Asian Earth Sci.* 176, 129–140. doi:10.1016/j.jseaes.2019.02.010

Matthews, M. V., and Reasenberg, P. A. (1988). Statistical methods for investigating qui escence and other temporal seismicity patterns. *Pure Appl. Geophys.* 126, 357–372. doi:10.1007/BF00879003

Mendoza, M. M., Ghosh, A., and Rai, S. S. (2016). Dynamic triggering of small local earthquakes in the central Himalaya. *Geophys. Res. Lett.* 43, 9581–9587. doi:10.1002/2016GL069969

Neves, M., Custodio, S., Peng, Z., and Ayorinde, A. (2018). Earthquake triggering in southeast africa following the 2012 Indian Ocean earthquake. *Geophys. J. Int.* 212, 1331–1343. doi:10.1093/gji/ggx462

Peng, Z., and Chao, K. (2008). Non-volcanic tremor beneath the central range in taiwan triggered by the 2001 Mw 7.8 kunlun earthquake. *Geophys. J. Int.* 175, 825–829. doi:10.1111/j.1365-246x.2008.03886.x

Peng, Z., Hill, D. P., Shelly, D. R., and Aiken, C. (2010a). Remotely triggered microearthquakes and tremor in central California following the 2010M_w8.8 Chile earthquake: Remote triggering in central California. *Geophys. Res. Lett.* 37, L24312. doi:10.1029/2010GL045462

Peng, Z., Vidale, J. E., Wech, A. G., Nadeau, R. M., and Creager, K. C. (2009). Remote triggering of tremor along the san Andreas Fault in central California. *J. Geophys. Res. Solid Earth* 114, B00A06. doi:10.1029/2008JB006049

Peng, Z., Wang, W., Chen, Q., and Jiang, T. (2010b). Remotely triggered seismicity in north China following the 2008 Mw 7.9 Wenchuan earthquake. *Earth Planets Space* 62, 893–898. doi:10.5047/eps.2009.03.006

Prakash, R., Singh, R. K., and Srivastava, H. N. (2016). Nepal earthquake 25 April 2015: Source parameters, precursory pattern and hazard assessment. *Nat. Hazards Risk* 7 (6), 1769–1784. doi:10.1080/19475705.2016.1155504

Prejean, S. G., Hill, D. P., Brodsky, E. E., Hough, S. E., Johnston, M. J. S., Malone, S. D., et al. (2004). Remotely triggered seismicity on the United States west coast following the Mw 7.9 Denali fault earthquake. *Bull. Seismol. Soc. Am.* 94 (6B), S348–S359. doi:10.1785/0120040610

Rajendran, C. P., and Rajendran, K. (2001). Characteristics of deformation and past seismicity associated with the 1819 kutch earthquake, northwestern India. *Bull. Seismol. Soc. Am.* 91 (3), 407–426. doi:10.1785/0119990162

Rastogi, B. K., Kumar, S., and Agrawal, S. K. (2012). Seismicity of Gujarat. *Nat. Hazards* 65, 1027–1044. doi:10.1007/s11069-011-0077-1

Rastogi, B. K., Singh, A. P., Sairam, B., Jain, S. K., Kaneko, F., Segawa, S., et al. (2011). The possibility of side effects: The Anjar case, following the past earthquakes in Gujarat, India. *Seismol. Res. Lett.* 82 (1), 692–701. doi:10.1785/gssrl.82.1.692

Rinne, M. (2008). *Fracture mechanics and subcritical crack growth approach to model time-dependent failure in brittle rock*. Helsinki: Helsinki University of Technology. urn.fi/URN. 978-951-22-9435-0.

Rubinstein, J. L., Gomberg, J., Vidale, J. E., Wech, A. G., Kao, H., Creager, K. C., et al. (2009). Seismic wave triggering of nonvolcanic tremor, episodic tremor and slip, and earthquakes on Vancouver Island. *J. Geophys. Res. Solid Earth* 114, B00A01. doi:10.1029/2008JB005875

Savage, H., and Marone, C. (2008). Potential for earthquake triggering from transient deformations. *J. Geophys. Res. Solid Earth* 113, B05302. doi:10.1029/2007JB005277

Sibson, R. H. (1974). Frictional constraints on thrust, wrench, and normal faults. *Nature* 249, 542–544. doi:10.1038/249542a0

Singh, A. P., Mishra, O. P., Rastogi, B. K., and Kumar, S. (2013). Crustal heterogeneities beneath the 2011 Talala, Saurashtra earthquake, Gujarat, India source zone: Seismological evidence for neo-tectonics. *J. Asian Earth Sci.* 62, 672–684. doi:10.1016/j.jseaes.2012.11.017

Singh, A. P., and Mishra, O. P. (2015)., 661. Gujarat, India, 38–48. doi:10.1016/j.tecto.2015.07.032Seismological evidence for monsoon induced micro to moderate earthquake sequence beneath the 2011 Talala, Saurashtra earthquake, Gujarat, India*Tectonophysics*

Singh, A. P., Zhao, L., Kumar, S., and Mishra, S. (2016). Inversions for earthquake focal mechanisms and regional stress in the Kachchh rift basin, Western India: Tectonic implications. *J. Asian Earth Sci.* 117, 269–283. doi:10.1016/j.jseaes.2015.12.001

Tullis, J., Yund, R. A., and Farver, J. (1996). Deformation-enhanced fluid distribution in feldspar aggregates and implications for ductile shear zones. *Geology* 24, 63–66. doi:10.1130/0091-7613(1996)024<0063:defdif>2.3.co;2

Velasco, A. A., Hernandez, S., Parson, T., and Pankow, K. (2008). Global ubiquity of dynamic earthquake triggering. *Nat. Geosci.* 1, 375–379. doi:10.1038/ngeo204

Wang, B., Harrington, R., Liu, Y., Kaoand, H., and Yu, H. (2019). Remote dynamic triggering of earthquakes in three unconventional Canadian hydrocarbon regions based on a multiple-station matched-filter approach. *Bull. Seismol. Soc. America109* 109, 372–386. doi:10.1785/0120180164

Wessel, P., Smith, W. H. F., Scharroo, R., Luis, J., and Wobbe, F. (2013). Generic mapping tools: Improved version released. *Am. Geophys. Union* 94 (45), 409–410. doi:10.1002/2013EO450001

Wu, C., Peng, Z., Wang, W., and Chen, Q. (2011). Dynamic triggering of shallow earthquakes near Beijing, China. *Geophys. J. Int.* 185 (3), 1321–1334. doi:10.1111/j.1365-246X.2011.05002.x

Wu, J., Peng, Z., Wang, W., Gong, X., Chen, Q., and Wu, C. (2012). Comparisons of dynamic triggering near Beijing, China, following recent large earthquakes in Sumatra. *Geophys. Res. Lett.* 39, L21310. doi:10.1029/2012GL053515

Yadav, R., Papadimitriou, E., Karakostas, V., Shanker, D., Rastogi, B., Chopra, S., et al. (2011). The 2007 Talala, Saurashtra, Western India earthquake sequence: Tectonic implications and seismicity triggering. *J. Asian Earth Sci.* 40 (1), 303–314. doi:10.1016/j.jseaes.2010.07.001

Yao, D., Peng, Z., and Meng, X. (2015). Remotely triggered earthquakes in south-central tibet following the 2004 Mw 9.1 Sumatra and 2005 Mw 8.6 nias earthquakes. *Geophys. J. Int.* 201 (2), 543–551. doi:10.1093/gji/ggv037